

## Soft X-ray Continuum Radiation From Low-Energy Pinch Discharges of Hydrogen

R. Mills<sup>1,a</sup>, R. Booker<sup>2</sup>, Y. Lu<sup>1</sup>

<sup>1</sup>BlackLight Power, Inc., 493 Old Trenton Road, Cranbury, NJ 08512, USA

<sup>2</sup>University of North Carolina, Asheville, NC 28804, USA

*Abstract*—Under a study contracted by GEN3 Partners, spectra of high current pinch discharges in pure hydrogen and helium were recorded in the EUV region at the Harvard Smithsonian Center for Astrophysics (CfA) in an attempt to reproduce experimental results published by BlackLight Power, Inc. (BLP) showing predicted continuum radiation due to hydrogen in the 10–30 nm region. Alternative explanations were considered to the claimed interpretation of the continuum radiation as being that emitted during transitions of H to lower-energy states (hydrinos). Continuum radiation was observed at CfA in the 10–30 nm region that matched BLP's results. Considering the low energy of 5.2 J per pulse, the observed radiation in the energy range of about 120 eV to 40 eV, reference experiments and analysis of plasma gases, cryofiltration to remove contaminants, and spectra of the electrode metal, no conventional explanation was found in the prior or present work to be plausible including contaminants, electrode metal emission, and Bremsstrahlung, ion recombination, molecular or molecular ion band radiation, and instrument artifacts involving radicals and energetic ions reacting at the CCD and H<sub>2</sub> re-radiation at the detector chamber. Moreover, predicted selective extraordinarily high-kinetic energy H was observed by the corresponding Doppler broadening of the Balmer  $\alpha$  line.

Key Words: plasma generation, plasma measurements, plasma pinch, spectroscopy, hydrogen

---

<sup>a</sup> Corresponding author: 609-490-1090 (phone); 609-490-1066 (fax); rmills@blacklightpower.com

## I INTRODUCTION

BlackLight Power, Inc. (BLP) reported the observation of EUV continuum radiation from a pinch gas discharge in the presence of molecular  $H_2$  in the discharge chamber [1–3] assigned to transitions to hydrino states (Sec. IIID). Spectra were measured with a vacuum grazing incidence spectrometer and recorded with a back-illuminated CCD camera. The gas pressure was varied in the range of 0.1 to 1.3 Torr. The spectrometer calibrated with O (and He) lines showed reliable wavelength measurements. BLP funded a study contracted by GEN3 Partners, Boston, MA to attempt reproducing the spectral measurements at the Harvard Smithsonian Center for Astrophysics, Cambridge, MA, USA (CfA) and the evaluation of possible alternative explanations by plasma physicist A. Bykanov [4]. In the present work, further studies were conducted by physicist R. Booker, Professor of Physics at the University of North Carolina at Asheville, and the other authors, using the experimental apparatus housed at BLP to investigate the mass spectrometer make-up of the gases being used in the experiment to search for possible contaminants that may lead to the observed continua. Visible spectra of the gas discharges being used were also taken. With all other possibilities eliminated, the continuum emission was certainly arising from hydrogen gas with W, Ta, and Mo electrodes. Further direct scrutiny of electrode plasma emission as the source of the continuum radiation was performed and this source was directly eliminated by recording the high resolution visible tungsten spectra on hydrogen and helium plasmas maintained with W electrodes and spectra of W plasmas formed by adding the metal as gaseous  $W(CO)_6$  volatilized by heating an open chamber containing the solid that was placed inside of the plasma cell. Moreover, the selective formation of high kinetic energy H atoms in excited states as observed by broadened Balmer emission was also studied to test additional theoretical predictions of the formations of hydrinos beyond the predicted unique continuum radiation.

## II. EXPERIMENTAL METHOD

### A. EUV Pinch Plasma Spectra

The BLP light source loaned to CfA and the experimental set up for recording the EUV spectra of pulsed plasmas using molybdenum (Mo), tantalum (Ta), and tungsten (W) electrodes are shown in Figures 1 and 2 with auxiliary systems shown in Figures 3A-B. These electrodes and test equipment including the high-voltage supplies, turbo pumps, back-illuminated CCD and CCD data processing equipment were also provided by BLP. Spectra of EUV radiation emitted from pure helium and pure hydrogen plasmas were recorded at CfA using CfA supplied UHP (Ultra High Purity) helium and hydrogen gas supplies. Additional spectra were recorded for helium-hydrogen mixtures at BLP. The spectra were recorded at CfA using a BLP-loaned

McPherson grazing incidence EUV spectrometer (Model 248/310G) equipped with a platinum-coated 600 g/mm or a platinum-coated 1200 g/mm grating. The angle of incidence was 87°. The wavelength resolution was about 0.05 nm with an entrance slit width of <1  $\mu\text{m}$ . The EUV light was detected by a CCD detector (Andor iDus) cooled to -60 °C. In addition, CfA provided a McPherson 248/310G spectrometer with a platinum-coated 1200 g/mm and a 133 g/mm grating. Both spectrometers and all CfA and BLP gratings were used as part of the measurement program as indicated in captions for Figures 4A-D.

The main BLP discharge cell comprised a hollow anode (3 mm bore) and a hollow cathode (3 mm bore) with electrodes made of Mo, Ta, or W (see Figure 1). The electrodes were separated by a 3 mm gap. A high voltage DC power supply was used to charge a bank of twenty 5200 pF capacitors connected in parallel to the electrodes. The cathode was maintained at a voltage of -10 kV before the triggering, while the anode was grounded. In some experiments, the voltage was increased up to -15 kV and decreased to -7 kV to determine the influence of this parameter on the observed spectra. An electron gun (Clinton Displays, Part # 2-001), driven by a high voltage pulse generator (DEI, PVX 4140), provided a pulsed electron beam with electron energy of 1-3 keV and pulse duration of 0.5 ms. The electron-beam triggered a high voltage pulsed discharge at a repetition rate of 5 Hz. The discharge was also self-triggered to determine the influence of the electron-beam on the spectral emission, and the electron-beam triggered repetition rate was varied between 1 and 5 Hz to determine if the electrode metal was the source of the continuum by varying the electrode temperature and vaporization rate.

Radiation was measured through an aperture that limited the gas flow from the discharge chamber into the detector chamber. Two-stage differential pumping resulted in low gas pressure in the detector chamber (in the range of 1E-6 Torr) while the gas pressure in the discharge chamber was maintained in the range from 0.1 to 1.3 Torr.

In all cases (BLP and CfA experiments), the BLP discharge cell was aligned with the spectrometer using a laser. The CCD detector was gated synchronously with the e-beam trigger. It had an exposure time of 100 ms for each discharge pulse having a breakdown time of about 300 ns. Each recorded spectrum accumulated radiation from 500 or 1000 discharges and in one case 5000 discharges. The CCD dark count was subtracted from the accumulated spectrum. The wavelength calibration was confirmed by OV and OVI lines from the oxygen present on the electrodes in the form of metal oxides. Typical flow rates of ultrahigh purity helium, hydrogen, and mixtures (at BLP), deuterium (at BLP), oxygen (at BLP), and oxygen-hydrogen mixtures (at BLP) ranged from 1 to 10 sccm, and the pressures in the discharge chamber were maintained between 100 mTorr and 1300 mTorr controlled by a mass flow controller (MKS). Both on-line mass spectroscopy and visible spectroscopy were used for monitoring contaminants in the plasma forming gases (BLP).

Additional experiments were conducted at BLP to test issues regarding conventional explanations of the radiation, to analyze mass and visible spectroscopy data for possible contaminants in the gases used, and to record the plasma emission of the electrode material under the same pressure, energy, and power conditions as the hydrogen plasmas (Sections IIIB, IIIC). Plasmas in pure oxygen (90 mTorr) and oxygen-hydrogen mixtures (total pressure ~300 mTorr) were measured for testing oxygen emission due to the oxide coating on the electrodes and for hydroxyl radicals, respectively. Using a common set of W-electrodes, the EUV spectra of helium-hydrogen mixtures (100% to 17%) were recorded to demonstrate the emission on a common intensity scale. Hydrogen at increasing pressure over the range of 2.2 mTorr to 16 mTorr was flowed into the EUV detector chamber while the EUV spectra of pure helium and pure hydrogen were recorded to verify possible artifacts involving H<sub>2</sub> re-radiation and H-radical recombination on the detector surface. The pure helium and pure hydrogen EUV spectra were recorded using an Aluminum (Al) (150 nm thickness, Luxel Corporation) or a polyimide filter (110 nm thickness, Luxel Corporation) to demonstrate that the soft X-rays are emitted from the plasma and exclude a possible instrumental artifact involving radicals or energetic ions reacting at the CCD. The hydrogen gas pressure in the CCD detector chamber was monitored using a Varian Thermocouple pressure gauge. The CCD detector position in the beam dispersed by the grating was changed from being centered at 20 nm to 10 nm to determine the short-wavelength cutoff of the hydrogen continuum radiation using the 600 g/mm grating and Ta electrodes.

### *B. Contaminant and Cryofiltered Gas Spectra*

Visible spectra were recorded using an Ocean Optics S2000 fiber optics spectrometer (with spectral band from 400 to 700 nm), and mass spectrometer data were acquired using the residual gas analyzer (RGA) while the plasma gases were being discharged and the EUV spectra simultaneously recorded. Figure 3A shows the experimental setup for taking the visible spectra and the mass spectra. The effect of the possible contaminants air, N<sub>2</sub>, O<sub>2</sub>, H<sub>2</sub>O, and low pressure Ar were studied by recording the effect on the hydrogen continuum with addition of these gases to the hydrogen plasma as well as the spectra of these gases in the absence of hydrogen. In addition, a liquid nitrogen cryotrap was added on-line to the EUV discharge in order to freeze out any liquid-nitrogen condensable contaminants that might be present in the hydrogen gas. The intensity of the continuum due to the cryotrap processing of the pure H<sub>2</sub> plasma gas was compared to that using H<sub>2</sub> without the cryotrap in place.

### *C. Electrode Metal Spectra*

High resolution visible spectra were recorded on pinch discharges with a Jobin Yvon Horiba 1250 M spectrometer (Figure 3A and described further below) on plasmas of the W electrode

metal formed by adding the metal as gaseous  $W(CO)_6$  volatilized by heating an open chamber containing the solid that was placed inside of the plasma cell while the EUV spectra were simultaneously recorded with the McPherson grazing incidence EUV spectrometer. Specifically, using an argon-filled glove box, approximately 0.5 g of  $W(CO)_6$  was loaded into a chamber comprising a 0.635 cm OD by 5 cm long stainless steel tube having one end sealed and the other end pressed to a narrow orifice of about 1 mm diameter. The chamber was placed in the discharge cavity behind the cathode. The plasma was initiated with either  $CO_2$  (100 mTorr) or  $N_2$  (130 mTorr) carrier gas where after energetic cations flying behind the cathode heated the tube to cause vaporization of  $W(CO)_6$ . To control for the C and O and N introduced with the metal atoms, EUV spectra were recorded on  $CO_2$  and  $N_2$  plasmas run at 100 mTorr and 130 mTorr, respectively.

#### *D. ToF-SIMS Spectra*

Time of flight secondary ion mass spectroscopy (ToF-SIMS) was performed on Mo and W foils using a Physical Electronics TFS-2000 ToF-SIMS instrument. The primary ion gun utilized a  $^{69}Ga^+$  liquid metal source. A region on each sample of  $(60 \mu m)^2$  was analyzed. In order to remove surface contaminants and expose a fresh surface, the samples were sputter-cleaned for 60 seconds using a  $180 \mu m \times 100 \mu m$  raster. The aperture setting was 3, and the ion current was 600 pA resulting in a total ion dose of  $10^{15}$  ions/cm<sup>2</sup>. During acquisition, the ion gun was operated using a bunched (pulse width 4 ns bunched to 1 ns) 15 kV beam. The total ion dose was  $10^{12}$  ions/cm<sup>2</sup>. Charge neutralization was active, and the post accelerating voltage was 8000 V. Representative post sputtering data is reported.

#### *E. Balmer Line Broadening Measurements*

The widths of the 656.3 nm Balmer  $\alpha$  line emitted from hydrogen plasmas and, as a comparison, the 667.82 nm He I line from helium plasmas with trace  $H_2$  were recorded to determine the neutral atomic temperature. The plasma emission was fiber-optically coupled to a Jobin Yvon Horiba 1250 M spectrometer through a high-quality UV (200-800 nm) fiber-optic bundle and a 220F matching fiber adapter with an aperture of 0.12 and a corresponding acceptance angle of 12°. The spectrometer had a 1250 mm focal length with a 2400 g/mm grating and a detector comprising a Symphony model, liquid-nitrogen cooled, back illuminated 2048×512 CCD array with an element size of  $13.5 \mu m \times 13.5 \mu m$ , 16 bit ADC, and 20 KHz and 1 MHz read outs. Using the 546 nm Hg I line from a NIST calibrated mercury lamp with the entrance and exit slits set to 20  $\mu m$ , the measured CCD resolution due to the finite-pixel-spectral width was very high,  $\pm 0.006$  nm. The spectrometer accuracy was  $\pm 0.05$  nm, and its repeatability was  $\pm 0.005$  nm. In each case, the spectrometer was scanned through the emission profile of the Balmer line or the

667.82 nm He I line with a step size of 0.01 nm and a 100 s and 50 s integration time, respectively.

### III. BASIC EXPERIMENTAL RESULTS

#### *A. EUV Pinch Plasma Spectra*

Spectra of discharges in high purity helium were measured as reference for validation of the continuum-free spectra in absence of hydrogen in a manner similar to that of BLP [1–3]. The EUV spectra of electron-beam-initiated, high-voltage pulsed gas discharges in helium using different electrodes, gratings, spectrometers, and numbers of CCD image superpositions are shown in Figures 4A-D. The known helium ion lines were observed in the absence of any continuum radiation. Oxygen ion lines were also observed similarly in all spectra including those from hydrogen discharges also shown in Figures 4A-D due to the oxide layer on the metal electrodes. In contrast to the helium spectra, the continuum band was observed when pure hydrogen was discharged. The emission spectra of electron-beam-initiated, pinch discharges in pure hydrogen recorded by the EUV grazing incidence spectrometer with Mo, Ta, and W electrodes and different gratings, spectrometers, and numbers of CCD image superpositions are shown in Figures 4A-D. Continuum radiation was observed from the hydrogen discharge regardless of the electrode material, spectrometer, or grating; although, the intensity of the emission from Mo electrodes was weaker than that of Ta and W at the short wavelengths possibly due to the associated plasma conditions that impact at least one of the continuum mechanism and intensity. However, it was found that the continuum width and features of the spectra became easily discernible as being from the same emitter independent of the electrode material by increasing the spectral intensity when using a more efficient grating and an increased the number of superpositions. The continuum is not attributed to oxygen ions or hydroxyl radicals as shown in Figures 5A and 5B, respectively. No continuum was observed from the pure oxygen discharge; but the continuum appeared in mixtures of O<sub>2</sub> and H<sub>2</sub> having intensity proportional to the hydrogen partial pressure. This dependency of the continuum intensity on the H<sub>2</sub> pressure was also observed in helium-hydrogen mixtures. As shown in Figure 6, the continuum intensity increased with hydrogen concentration in helium-hydrogen mixtures, and the spectrum approached that of pure hydrogen at high H<sub>2</sub> concentration further eliminating electrode metal lines as the source of the continuum. Figures 4-7 show that the hydrogen continuum radiation comprises two profiles, one with a short wavelength cutoff at about 10 nm and a second is distinguishable by a reversal of the slope of the intensity versus wavelength in the region of 22-23 nm. Conventional mechanisms of the continuum radiation unique to hydrogen in a region wherein hydrogen was previously not known to emit were sought.

Specific known mechanisms were previously evaluated [4] using data from the literature and the input of further test data from BLP. Electrode metal emission was indirectly eliminated since the spectral features were the same over any given region where it was intense enough to be detected using different electrodes, and the intensity was shown to be proportional to concentration of hydrogen. Recombination and Bremsstrahlung mechanisms were excluded because the intensities of these types of continuum spectra scale with  $Z$  as  $Z^2$  or  $Z^4$ , respectively. Thus, we should have observed a more intense continuum spectrum in He ( $Z=2$ ) than in  $H_2$  ( $Z=1$ ). The applied pulsed voltage to drive the plasma was increased from -10 kV to -15 kV and decreased to -7 kV in sequential runs to determine any high-energy electron effect on the spectral profile. No effect was observed; thus, high-energy electrons were eliminated as a possible cause of continuum radiation. Figure 8 shows a self-triggered spectrum using hydrogen gas, showing the presence of the continuum. Without an electron beam trigger, the continuum is still present for hydrogen. This eliminates the influence of the electron beam as the source of the continuum. Band radiation for molecular electronic transitions broadened by vibrational and rotational transitions including hydrogen molecular or molecular ion emission cannot be the source due to the extraordinary energy ( $>100$  eV) of the continuum radiation compared to the energy levels of these species. Another reason for excluding this mechanism is the broad energy width of the continuum band ( $\sim 60$  eV) that cannot be explained by the current plasma temperature (max 15 eV, most likely  $<10$  eV). By using spectral-region-cutoff filters and recording the spectral profile change with changing of the CCD position (Figure 9), the source of the continuum radiation was confirmed to be the hydrogen plasma, and the emission was deemed a true spectrum. Addition of hydrogen gas to the CCD chamber had no effect on the emission profile. These results eliminated detection artifacts as possibilities. In summary, considering the low energy of 5.2 J per pulse, the observed radiation in the photon energy range from 40 eV to 120 eV, and reference experiments with He and oxygen and other common contaminants, no conventional explanation was found to be plausible including electrode metal emission, Bremsstrahlung, ion recombination, molecular or molecular ion band radiation, and instrument artifacts involving radicals and energetic ions reacting at the CCD and  $H_2$  re-radiation at the detector.

Summarizing the basic spectral measurements, we may formulate the following:

1. The CCD camera records some signal attributed to a continuum spectrum ranging from 10 to 30 nm only in presence of  $H_2$ . No continuum was observed for neat He gas or other gases tested.
2. The intensity of the continuum spectrum scales proportionally to  $H_2$  concentration in the mixture with He or  $O_2$ .

3. The width of the continuum, but not its presence, depends on the grating and electrode material. When the continuum radiation was observed with high intensity over the region 10-30 nm, it appeared that two bands were present.
4. Energetic electrons from the electron gun and the electron beam as agents influencing the continuum band were eliminated.
5. Spectra taken with an Al filter each exhibit a sharp edge on the continuum band corresponding to the transmission edge of the filter.
6. The continuum was not due to a detection artifact.

Comparing these and other reported results [1–3], it can be appreciated that the CfA group reproduced the published results of BlackLight Power, Inc. [4]. Continuum radiation was observed from pure hydrogen over the spectral region ~10 to 30 nm; whereas, no continuum was observed from helium plasmas run under essentially identical conditions. Only helium ion and background oxygen ion emission were observed; wherein, the latter was common to both plasma sources. By comparing all hydrogen results involving different electrodes, gratings, spectrometers, and numbers of CCD image superpositions, it was concluded that the same emitter was common in all cases of hydrogen continuum emission. Any variation in the observed spectral range in the region 10 nm to 30 nm may depend on the sensitivity of the detection and plasma conditions that influence the emission. The hydrogen continuum radiation comprised two profiles, one with a short wavelength cutoff at about 10 nm and a second was distinguishable by a reversal of the slope of the intensity versus wavelength in the region of 22-23 nm. Other than emission from hydrogen, the only other possibilities not completely exhausted were some unknown gas contaminant or emission from the electrodes since these were the only other potential emitters present. Given the significant implications of the observation of hydrogen emission in a high-energy region previously unknown, these possibilities were exhaustively scrutinized.

#### *B. Possible Artifact: Contaminants in Plasma Gases*

Contaminants in the hydrogen and hydrogen admixture plasma gases that produced the observed EUV continuum radiation were ruled out by the use of a visible spectrometer and a residual gas analyzer (RGA) mass spectrometer. There was no species found in the hydrogen gas that could give rise to such continuum emission. Only trace common contaminants were observed in the plasma gases. Figures 10A-B show mass spectra of the mass spectrometer chamber background and the H<sub>2</sub> pinch pulse plasma gas. The H<sub>2</sub> pinch pulse plasma gas mainly shows H<sub>2</sub><sup>+</sup>, H<sub>3</sub><sup>+</sup>, and H<sub>2</sub>O<sup>+</sup>. All the gases used were ultra high pure (UHP) gases. CfA spectroscopists conducted the pinch discharge experiments using their own cylinders of gas, different than the ones used by

BLP. Both the experiments at CfA and at BLP showed continua only for pure hydrogen and hydrogen gas mixtures, such as  $H_2 + O_2$ ,  $H_2 + N_2$ ,  $H_2 + Ar$ ,  $H_2 + H_2O$ , and  $H_2 + air$ . In contrast, no continuum was observed from any of these gases ( $O_2$ ,  $N_2$ ,  $Ar$ ,  $H_2O$ , and  $air$ ), with no hydrogen present. The same spectral results were observed even though both groups used completely different cylinders of gas. Pure contaminants  $air$ ,  $N_2$ ,  $O_2$ ,  $H_2O$ , and low pressure  $Ar$  did not produce a continuum in the EUV region.

The possibility that these gases were contaminants in the hydrogen was studied by recording the effect of intentionally adding the candidate contaminants to the hydrogen plasma gas. If the continuum was from one of these contaminant gases, then adding more of the contaminant should have caused an increase in the continuum. But, in all of these cases, adding these gases to hydrogen did not increase the intensity of the continuum compared to the continuum present with pure  $H_2$ . Figure 5B and Figures 4A-D show the EUV spectrum of a discharge with an  $H_2 + O_2$  mixture compared to the continuum from a discharge made only with  $H_2$ , showing that the intensity of the continuum is weaker with  $O_2$  with correspondingly less  $H_2$ . The continuum was observed to be emitted with hydrogen and hydrogen admixtures, but the continuum was no more pronounced than with hydrogen alone. So, the continuum was not caused by the reaction of  $H_2$  with the contaminants.

A liquid nitrogen (LN) cryotrap was placed in the gas line to the plasma chamber to condense any possible liquid-nitrogen condensable contaminants flowing into the plasma discharge gas stream as well as possible contaminants in the discharge chamber. No change in the intensity or spectral profile of the pure  $H_2$  continuum was observed due to the presence of the LN cryotrap. Figure 11A shows the RGA mass spectrometer data on the hydrogen gas used in the discharge using the LN cryotrap. It shows the same chemical species as in Figure 10B without the LN cryotrap. Figure 11B shows the EUV hydrogen discharge spectra using the liquid nitrogen cryotrap wherein the continuum was observed. For comparison, the continuum results of the  $H_2$  discharge without the LN cryotrap in place is shown in Figures 4A-D.

A group at Eindhoven University of Technology (TUE) replicated the hydrogen continuum emission from an independently constructed replica of the plasma source shown in Figures 1 and 2 that comprised Mo electrodes [5]. Their conclusion was that the only remaining explanation other than hydrinos was an unknown contaminant. The cryotrap and visible and mass spectroscopic studies address and resolve this remaining issue. Our conclusion is that this continuum exists only in the presence of hydrogen, and that it is not due to a contaminant gas in the hydrogen sample. The continuum was observed when hydrogen was added, but was also present when hydrogen or a source of hydrogen such as  $H_2O$  or hydrocarbons was in the background of other test gases or was off-gassed from metals as indicated by strong Balmer emission. When the background contamination was removed with pumping and heating, the

continuum was eliminated. This is an important consideration when repeating these results or considering historical spectra. Furthermore, since transitions to states  $H(1/p)$  ( $p > 4$ ) produces continuum radiation in shorter-wavelength regions of the spectrum, it may serve as a preferred light source of lithography and may be at least partially responsible for radiation generated by plasmas using hydrogen blanket gas, a common practice in the industry.

### *C. Possible Artifact: Electrode Emission*

The absence of the continuum or absence of an effect on the continuum by contaminant and control gases further confirm that the continuum is not due to the electrodes which were the same in all cases with common plasma parameters. The continuum is dependent only on the presence and the concentration of hydrogen. Further direct scrutiny of electrode plasma emission as the source of the continuum radiation was performed by recording the high resolution visible tungsten spectra on hydrogen and helium plasmas maintained with W electrodes and spectra of W plasmas formed by adding the metal as gaseous  $W(CO)_6$  volatilized by heating an open chamber containing the solid that was placed inside of the plasma cell. Emission spectra (5-50 nm) of electron-beam-initiated, high-voltage pulsed discharges in  $H_2$  compared to  $W(CO)_6$  with  $CO_2$  and  $N_2$  plasma maintenance gas and control He,  $CO_2$ , and  $N_2$  plasmas maintained with W electrodes are shown in Figures 12A-H. Only the  $H_2$  plasma showed a continuum in the EUV region and plasmas of He,  $CO_2$ ,  $N_2$ ,  $W(CO)_6$  in  $CO_2$ , and  $W(CO)_6$  in  $N_2$  showed no EUV continuum. Figure 13 shows the superimposed high-resolution visible emission spectra (400-402 nm) corresponding to the EUV spectra shown in Figures 12A-H wherein the line assignment was according to NIST [6]. The observed order of increasing intensity of the W I 400.87 nm line was  $H_2 < N_2 < CO_2 < He \ll W(CO)_6$  in  $N_2 < W(CO)_6$  in  $CO_2$ .  $H_2$  showed the lowest W emission consistent with its inefficiency as a sputtering species due to its low mass wherein the electrodes were the only source. The presence of C and N in plasmas comprising  $CO_2$  and  $N_2$  could form a protective tungsten carbide or nitride coating on the electrode to reduce the sputtering of the corresponding ions. The absence of continuum emission from all other sources having much greater W emission from the W electrodes and with added W from  $W(CO)_6$  directly indicate that W is not the source of the continuum emission. Rather hydrogen is the source.

Thus, it was observed that helium having no EUV continuum emission produced the W line emission from W electrodes at 10 times greater intensity than  $H_2$ . These results are consistent with the known physics of metal sputtering in plasmas wherein the bombardment of a metal with a higher mass ion (4 for  $He^+$  compared to 1 for  $H^+$ ) causes greater sputtering [7,8]. Furthermore, the observation of only W atomic emission and the absence of electrode metal ions in the visible region where a definite line assignment was made further eliminated the electrodes as the source of the continuum. The near absence of W visible emission in  $H_2$  plasmas makes it

virtually impossible that W can be the source of the continuum emission in the 10 to 30 nm region since no emitter can exclusively and selectively thermally emit in a constrained band of the EUV under these pinch plasma conditions. In fact, no W lines were observed in the EUV region of any plasma indicating that W is a weak emitter in the EUV. These results are consistent with the very weak W ion emission in the EUV observed even in plasmas of much higher energy such as those reported in the literature [9] regarding the injection of  $W(CO)_6$  into magnetically confined plasmas having temperatures of 25-100 eV compared to our pinch plasma having a likely temperature of less than 10 eV.

These results are also consistent with a further fundamental consideration regarding corrosion and metal vaporization by plasma gas. The anode is the electrode that actually shows any visibly observable erosion compared to the cathode. The high current of high-energy electrons at the anode is the major source of power dissipation in the pinch plasma. Thus, the nature of the cations is essentially irrelevant, and cations are repelled by the anode, especially as a function of decreasing mass due the relative ease of deflection. Again, it is counter to physical expectations that hydrogen should be more efficient at producing electrode metal vapor plasma than other heavier plasma gases run as controls. And, the visible W emission supports this premise.

Further testing was performed on the well-known sputtering efficiency dependence on the mass of the sputtering ion [7,8]. Consistently, Brauner [10] calculated the hydrogen sputter yield to be two orders of magnitude lower than that of xenon gas discharge plasmas. Thus, hydrogen should not give a continuum relative to other heavy ions tested, in contrast to observations. To determine if hydrogen is an exception to the rule, the electron-beam triggered repetition rate was varied between 1 and 5 Hz in order to vary the electrode temperature and vaporization rate as observed for xenon discharge plasmas, for example [10]. However, there was no increase in the hydrogen continuum intensity due to the higher repetition rate and commensurate higher electrode vaporization rate, in contrast to expectations if the electrode metal was the source of continuum. As an additional sputtering test, deuterium was substituted for hydrogen, and the higher mass hydrogen had no effect on the intensity of the continuum either. Thus, electrode metal sputtering with emission as the source of the continuum was ruled out.

Another remote possibility considered was that hydrogen causes a special chemical reaction that produces a protonated electrode metal ion from the heavy refractory metals used. Ion beams are a method of forming metal plasmas for metal continuum lithographic light sources [8]. ToF-SIMS combines an ion beam ( $Ga^+$  in this study) to form metal ions with high mass resolution for ion identification. Mo foil was another electrode material used to produce hydrogen continuum radiation in BLP, CfA, and TUE [5] studies wherein only weak Mo atomic

lines were observed in the visible. Independent observations have shown Mo not to emit continuum in the 10-30 nm region, even from plasmas at much higher energies [11]. We analyzed Mo foil by ToF-SIMS using gallium ion bombardment to form positive ions identified by the isotope peaks to 10,000 resolution to test the hypothesis of Mo forming a special protonated ion. No  $M + 1$  peak was observed for Mo; whereas, a strong  $M + 1$  peak was observed for Ti that was also present in the sample as an internal control comprising a metal that forms a hydride. Furthermore, the peak intensity was very low for Mo and barely discernible for W when it was run, consistent with the low production efficiency of positive ions with increasing mass since the amount of energy and momentum transferred from the incident gallium ion to the target atom is dependent on the mass ratio of ion and atom [12,13]. Again, no  $M + 1$  peak was observed. The results are consistent with the known thermodynamics of metal hydrides wherein  $\Delta H^\circ$ (kcal/mol H) for the hydrides of Ti, Mo, and W are -10.8, +12.3, and +5.0, respectively [14]. Thus, any special hydrogen chemistry involving the electrode material was eliminated.

#### D. Possible Explanation of Continua

Mills predicted that atomic hydrogen forms fractional Rydberg energy states  $H(1/p)$  called "hydrino atoms" wherein  $n = \frac{1}{2}, \frac{1}{3}, \frac{1}{4}, \dots, \frac{1}{p}$  ( $p \leq 137$  is an integer) replaces the well-known parameter  $n = \text{integer}$  in the Rydberg equation for hydrogen excited states [1–3, 15–18]. The transition of H to  $H\left[\frac{a_H}{p=m+1}\right]$  occurs by a nonradiative resonance energy transfer of  $m \cdot 27.2$  eV to  $m$  H atoms ( $m$  is an integer) to form an intermediate that decays with the emission of continuum bands with short wavelength cutoff and energies  $E_{\left(H \rightarrow H\left[\frac{a_H}{p=m+1}\right]\right)}$  given by

$$E_{\left(H \rightarrow H\left[\frac{a_H}{p=m+1}\right]\right)} = m^2 \cdot 13.6 \text{ eV} \quad \text{and} \quad \lambda_{\left(H \rightarrow H\left[\frac{a_H}{p=m+1}\right]\right)} = \frac{91.2}{m^2} \text{ nm} \quad (1)$$

and extending to longer wavelengths than the corresponding cutoff. This theory explains the photon energy range observed in the plasma emission experiments with molecular hydrogen.

Since the potential energy of atomic hydrogen is 27.2 eV, two atoms formed from  $H_2$  by collision with a third, hot H-atom can act as a catalyst for this third H by accepting  $2 \cdot 27.2$  eV from it. Similarly, the collision of two hot  $H_2$  molecules provide 3 H to serve as a catalyst of  $3 \cdot 27.2$  eV for the fourth. After the energy transfer to the catalyst, an intermediate is formed having the radius of the H atom and a central field of 3 and 4 times the central field of a proton, respectively. Furthermore, the radius is predicted to decrease as the electron undergoes radial acceleration to a stable state having a radius of 1/3 and 1/4 the radius of the uncatalyzed hydrogen atom, with the release of 54.4 eV and 122.4 eV of energy, respectively. This energy is

emitted as a characteristic EUV continuum with a cutoff at 22.8 nm and 10.1 nm, respectively, and extending to longer wavelengths. An alternative to the mechanism involving energetic molecular collisions to permit the multi-body interactions of H atoms to form hydrinos involves the creation of a highly dense H gas in the recombining pinch plasma that is supported by temporal evolution measurements of the continuum [3].

The hydrino transition reaction between three hydrogen atoms occurs when two atoms resonantly and nonradiatively accept 54.4 eV from the third hydrogen atom where 2H serve as the catalyst. The reaction proceeds in two steps of energy release:

$$54.4 \text{ eV} + 2\text{H} + \text{H} \rightarrow 2\text{H}_{fast}^+ + 2e^- + \text{H}^* \left[ \frac{a_H}{3} \right] + 54.4 \text{ eV} \quad (2)$$

$$\text{H}^* \left[ \frac{a_H}{3} \right] \rightarrow \text{H} \left[ \frac{a_H}{3} \right] + 54.4 \text{ eV} \quad (3)$$

$$2\text{H}_{fast}^+ + 2e^- \rightarrow 2\text{H} + 54.4 \text{ eV} \quad (4)$$

$$\text{H} \rightarrow \text{H} \left[ \frac{a_H}{3} \right] + [3^2 - 1^2] \cdot 13.6 \text{ eV} \quad (5)$$

where  $\text{H}^*[a_H/3]$  has the radius of the hydrogen atom plus a central field of 3 times that of a proton and  $\text{H}[a_H/3]$  is the corresponding stable state with the radius of 1/3 that of H. Here, the extreme-ultraviolet continuum radiation band due to the decay of the  $\text{H}^*[a_H/3]$  intermediate is predicted to have a short wavelength cutoff at  $E = m^2 \cdot 13.6 = 4 \cdot 13.6 = 54.4 \text{ eV}$  (22.8 nm) [where  $p = m + 1 = 3$  and  $m = 2$  in Eq. (1)] and extending to longer wavelengths.

In another H-atom catalyst reaction two hot  $\text{H}_2$  molecules collide and dissociate so that 3 H-atoms serve as the catalyst of  $3 \cdot 27.2 \text{ eV} = 81.6 \text{ eV}$  for the fourth H-atom. The reactions where three atoms resonantly and nonradiatively accept 81.6 eV from the fourth hydrogen atom such that 3H serves as the catalyst are given by:

$$81.6 \text{ eV} + 3\text{H} + \text{H} \rightarrow 3\text{H}_{fast}^+ + 3e^- + \text{H}^* \left[ \frac{a_H}{4} \right] + 81.6 \text{ eV} \quad (6)$$

$$\text{H}^* \left[ \frac{a_H}{4} \right] \rightarrow \text{H} \left[ \frac{a_H}{4} \right] + 122.4 \text{ eV} \quad (7)$$

$$3\text{H}_{fast}^+ + 3e^- \rightarrow 3\text{H} + 81.6 \text{ eV} \quad (8)$$

$$\text{H} \rightarrow \text{H} \left[ \frac{a_H}{4} \right] + [4^2 - 1^2] \cdot 13.6 \text{ eV} \quad (9)$$

Here the extreme-ultraviolet continuum radiation band due to the decay of the  $\text{H}^*[a_H/4]$  intermediate is predicted to have a short wavelength cutoff at  $E = m^2 \cdot 13.6 = 9 \cdot 13.6 = 122.4 \text{ eV}$  (10.1 nm) [where  $p = m + 1 = 4$  and  $m = 3$  in Eq. (1)] and extending to longer wavelengths. Another observation predicted by Eqs. (4) and (8) is the formation of fast, excited state H atoms from recombination of fast  $\text{H}^+$ . The fast atoms give rise to broadened Balmer  $\alpha$  emission. A

population of extraordinarily high-kinetic-energy hydrogen atoms in certain mixed hydrogen plasmas is a well-established phenomenon; however the mechanism has been controversial in that the conventional view that it is due to field acceleration is not supported by the data and critical tests [19–38]. Rather it is shown that the cause is due to the energy released in the formation of hydrinos [19–38]. Fast H was sought in continuum-emitting hydrogen pinch plasmas.

### *E. Broadened Balmer Emission*

The energetic hydrogen atom energies were calculated from the width of the 656.3 nm Balmer  $\alpha$  line emitted from hydrogen pinch plasmas. Each Balmer  $\alpha$  spectral line was fit using one or three Gaussian curves: one for the “cold” (<1 eV) hydrogen and two for “hot” (>10 eV) hydrogen. The full half-width  $\Delta\lambda_G$  of each Gaussian results from the Doppler ( $\Delta\lambda_D$ ) and instrumental ( $\Delta\lambda_I$ ) half-widths:

$$\Delta\lambda_G = \sqrt{\Delta\lambda_D^2 + \Delta\lambda_I^2} \quad (10)$$

The measured half-width  $\Delta\lambda_I$  of  $\pm 0.006$  nm was negligible. Thus, the temperature was calculated from the Doppler half-width using the formula:

$$\Delta\lambda_D = 7.16 \times 10^{-7} \lambda_0 \left( \frac{T}{\mu} \right)^{1/2} \quad (11)$$

where  $\lambda_0$  is the line wavelength,  $T$  is the temperature in K (1 eV = 11,605 K), and  $\mu$  is the molecular weight (=1 for atomic hydrogen). In each case, the average Doppler half-width that was not appreciably changed with pressure varied by  $\pm 5\%$ , corresponding to an error in the energy of  $\pm 10\%$ .

The 656.3 nm Balmer  $\alpha$  line widths recorded on the hydrogen and helium-hydrogen pinch plasmas are shown in Figures 14A-B. In each case, the Balmer  $\alpha$  line profile of the plasma emission comprised three distinct Gaussian peaks, an inner, narrower peak corresponding to a slow component of less than 1.5 eV and two outer, significantly broadened peaks. The energies of the corresponding fast components of the tri-modal distribution of neutral species temperatures of the H<sub>2</sub> plasma are 98 eV and 8.8 eV accounting for 18% and 33% of the  $n = 3$  excited-state H population. The energies of the corresponding fast components of the tri-modal distribution of neutral species temperatures of the He/trace H<sub>2</sub> plasma are 35 eV and 3.2 eV accounting for 7% and 26% of the  $n = 3$  excited-state H population. Only the hydrogen lines were broadened in the helium-hydrogen plasma as shown in Figures 14B and 15. The Doppler half-width of the 667.82 nm He I line as shown in Fig. 10 is 0.025 nm, and it can be accurately resolved by the high-resolution spectrometer with an instrumental half-width of only 0.006 nm.

The He atoms' average thermal energy corresponding to a 0.025 nm Doppler half-width is 0.98 eV.

The narrow line width of the He I line (Figure 15) indicates that Stark broadening can be disregarded without loss of accuracy. A possible conventional mechanism for excessive  $H_\alpha$  Gaussian line width in pure hydrogen and mixtures of hydrogen with helium [19–38] corresponding to Doppler broadening is the formation of energetic ions ( $H^+$ ,  $H_2^+$  and  $H_3^+$ ) by electric field acceleration followed by energy transfer to the matrix gas (H and  $H_2$ ) through charge exchange collisions. However, the mechanism fails to predict the selective transfer of energy to the hydrogen atomic excited state with the helium atoms of the admixed gases remaining cold ( $<1$  eV) even when the mass ratios are comparable (Figure 15). Furthermore, this field-acceleration mechanism can only account for the red portion of the spectrum when viewed optically towards the ion-accelerating electrode. Thus, it fails to explain how the observed enhanced blue-shifted  $H_\alpha$  spectra width is symmetric with respect to the red-shifted portion of the emission profile (Figures 14A-B). Consistent with prior analyses [19–25], the selective formation of energetic hydrogen is explained by the energy released in the reactions to form hydrinos given by Eqs. (4) and (8) and others to even lower-energy states.

#### IV. CONCLUSION

The continuum radiation was observed at BLP and CfA in the 10–30 nm region that comprised two continua bands with one having a short wavelength cutoff at about 10 nm and a second continuum was identifiable as a slope change on the first at about 23 nm. Considering the low energy of 5.2 J per pulse, the observed radiation in the energy range of about 120 eV to 40 eV, and reference experiments with He and other gases, no conventional explanation was found to be plausible including electrode metal emission, Bremsstrahlung, ion recombination, molecular or molecular ion band radiation, and instrument artifacts involving radicals and energetic ions reacting at the CCD and  $H_2$  re-radiation at the detector chamber. Additionally, contaminant and electrode vapor emission as the source of the continuum was directly eliminated by (i) running EUV spectra of laboratory and possible gas contaminants wherein pure contaminants air,  $N_2$ ,  $O_2$ ,  $H_2O$ , and low pressure Ar did not produce the continuum, (ii) recording the visible and mass spectra on hydrogen gas that produced continua showing the absence of a contaminant source of continuum, (iii) eliminating possible contaminants using a cryotrap on hydrogen plasmas, (iv) recording the high resolution visible spectra of hydrogen and helium plasmas maintained with W electrodes wherein it is was observed that helium having no EUV continuum emission produced 10 times greater intensity W visible emission than hydrogen, and (v) simultaneously recording

EUV and visible emission on W metal plasmas introduced as a metal carbonyl gas that directly eliminated the W electrodes as the source of the continuum.

In summary:

- A.) There is continuum radiation in the EUV region that is only observed with hydrogen and hydrogen mixtures with other gases, but which is not observed with helium or other gases by themselves without hydrogen.
- B.) This is actual radiation from the plasma and is not induced by artifacts in the detector.
- C.) The continuum spectrum cannot be explained by recombination spectra, Bremsstrahlung or molecular or molecular ion (e.g.  $\text{H}_2^+$ ) transitions. It cannot be the result of the electron trigger since the continuum is still present in the absence of electron triggering.
- D.) Contaminants in the gases producing this continuum radiation can be ruled out since we showed only trace amounts were present by the use of RGA mass spectroscopy and visible spectra. Furthermore, pure contaminants air,  $\text{N}_2$ ,  $\text{O}_2$ ,  $\text{H}_2\text{O}$ , and low pressure Ar did not give rise to such a continuum.
- E.) The continuum emission was not due to electrode emission since it depended only on hydrogen, occurred with three different electrode materials, was absent from a plasma comprised of the electrode material supplied as gaseous  $\text{W}(\text{CO})_6$ , and the corresponding ions that have emission in the EUV region were absent even in hydrogen plasmas as shown by the visible spectra. It has been shown in the literature that W is a weak EUV emitter even at significantly higher energies and does not emit continuum radiation [9].

A match with all of the observations is that the product is  $\text{H}(1/p)$ , fractional Rydberg states of atomic hydrogen called “hydrino atoms” wherein  $n = \frac{1}{2}, \frac{1}{3}, \frac{1}{4}, \dots, \frac{1}{p}$  ( $p \leq 137$  is an integer) replaces the well-known parameter  $n = \text{integer}$  in the Rydberg equation for hydrogen excited states. Similar to excited state H, each atomic hydrino state also comprises an electron, a proton, and a photon, but the field contribution from the photon increases the binding rather than decreasing it corresponding to energy desorption rather than absorption. Since the potential energy of atomic hydrogen is 27.2 eV, one or more ( $m$ ) H atoms can act as a catalyst for a given H by accepting  $m \cdot 27.2$  eV from it. Following the nonradiative energy transfer, further energy as characteristic continuum radiation having a short-wavelength cutoff of  $m^2 \cdot 13.6$  eV is released as the hydrino transitions to a final stable radius of  $1/(1+m)$  that of H. Thus, the characteristic continuum radiation having a short-wavelength cutoff of  $m^2 \cdot 13.6$  eV matched that predicted for hydrino transitions. The transition also produced predicted selective extraordinary high-kinetic energy H that was observed by the corresponding broadening of the Balmer  $\alpha$  line.

H<sub>2</sub> (1/4) The discovery of high-energy continuum radiation from hydrogen as it forms a more stable form has astrophysical implications such as hydrino being a candidate for the identity of dark matter and the corresponding emission being the source of high-energy celestial and stellar continuum radiation [1,2]. For example, the EUV spectra of white dwarfs matches the profile shown in Figures 4A-D. Other prior inexplicable laboratory observations may also be resolved due to this discovery of hydrinos [16].

#### REFERENCES

- [1] R. L. Mills, Y. Lu, “Hydrino continuum transitions with cutoffs at 22.8 nm and 10.1 nm,” *Int. J. Hydrogen Energy*, 35 (2010), pp. 8446-8456, doi: 10.1016/j.ijhydene.2010.05.098.
- [2] R. L. Mills, Y. Lu, K. Akhtar, “Spectroscopic observation of helium-ion- and hydrogen-catalyzed hydrino transitions,” *Cent. Eur. J. Phys.*, 8 (2010), pp. 318-339, doi: 10.2478/s11534-009-0106-9.
- [3] R. L. Mills, Y. Lu, “Time-resolved hydrino continuum transitions with cutoffs at 22.8 nm and 10.1 nm,” *Eur. Phys. J. D*, 64, (2011), pp. 63, DOI: 10.1140/epjd/e2011-20246-5.
- [4] A. Bykanov, “Validation of the observation of soft X-ray continuum radiation from low energy pinch discharges in the presence of molecular hydrogen,” [http://www.blacklightpower.com/pdf/GEN3\\_Harvard.pdf](http://www.blacklightpower.com/pdf/GEN3_Harvard.pdf).
- [5] A. F. H. van Gessel, Masters Thesis: *EUV spectroscopy of hydrogen plasmas*, April (2009), Eindhoven University of Technology, Department of Applied Physics, Group of Elementary Processes in Gas Discharges, EPG 09-02, pp. 61-70.
- [6] NIST Atomic Spectra Database, [www.physics.nist.gov/cgi-bin/AtData/display.ksh](http://www.physics.nist.gov/cgi-bin/AtData/display.ksh).
- [7] D. S. Finley, S. Bowyer, F. Paresce, R. F. Malina, “Continuous discharge Penning source with emission lines between 50 Å and 300 Å,” *Appl. Optics*, (1979), Vol. 18, No. 5, pp. 649–654.
- [8] F. Watt, A. A. Bettiol, J. A. Van Kan, E. J. Teo, M. B. H. Breese, “Ion beam lithography and nanofabrication: a review”, *International J. of Nanoscience*, Vol. 4, No. 3, (2005), pp. 269-286.
- [9] J. Clementson, P. Beiersdorfer, E.W. Magee, H. S. McLean, R.D. Wood, “Tungsten spectroscopy relevant to the diagnostics development of ITER divertor plasmas”, *J. Phys. B*, Vol. 43, (2010), pp. 144009.
- [10] T. Brauner, Doctoral Thesis: *Particle Emission from Extreme Ultraviolet Light Sources*, Friedrich-Schiller University Jena, Faculty of Physics and Astronomy, pp. 69-72.

- [11] M. B. Chowdhuri, S. Morita, M. Goto, "Line analysis of EUV spectra from molybdenum and tungsten injected with impurity pellets in LHD", 16th International Toki Conference, Toki Japan, December 5-8, 2006.
- [12] T. Grehl, "Improvement in TOF-SIMS Instrumentation for Analytical Application and Fundamental Research", Inaugural-Dissertation zur Erlangung des Doktorgrades der Naturwissenschaften im Fachbereich Physik der Mathematisch-Naturwissenschaftlichen Fakultät der Westfälischen-Wilhelms Universität Münster, (2003).
- [13] L. A. Giannuzzi, B. I. Prenitzer, B. W. Kempshall, *Introduction to Focused Ion Beams Instrumentation, Theory, Techniques and Practice*, L. A. Giannuzzi, F. A. Stevie, Editors, (Springer, New York, NY, 2005), Chapter 2, Ion-Solid Interactions, pp. 13-52.
- [14] H. M. Lee, "The solubility of hydrogen in transition metals", *Metallurgical Transactions A*, Vol. 7A, (1976), pp. 431-433.
- [15] R. Mills, *The Grand Unified Theory of Classical Physics*; July 2010 Edition, posted at <http://www.blacklightpower.com/theory/bookdownload.shtml>.
- [16] R. L. Mills, J. Lotoski, G. Zhao, K. Akhtar, Z. Chang, J. He, X. Hu, G. Wu, G. Chu, Y. Lu, "Identification of new hydrogen states," *Physics Essays*, Vol. 24 (2011), pp. 95-116.
- [17] R. L. Mills, G. Zhao, K. Akhtar, Z. Chang, J. He, X. Hu, G. Wu, J. Lotoski, G. Chu, "Thermally reversible hydrino catalyst systems as a new power source," *Int. J. Green Energy*, 8 (2011), 429-473.
- [18] R.L. Mills, K. Akhtar, G. Zhao, Z. Chang, J. He, X. Hu, G. Chu, "Commercializable power source using heterogeneous hydrino catalysts," *Int. J. Hydrogen Energy*, Vol. 35 (2010), pp. 395-419, doi: 10.1016/j.ijhydene.2009.10.038.
- [19] K. Akhtar, J. Scharer, R. L. Mills, "Substantial Doppler broadening of atomic-hydrogen lines in DC and capacitively coupled RF plasmas," *J. Phys. D, Applied Physics*, Vol. 42, (2009), 42 135207 (2009) doi:10.1088/0022-3727/42/13/135207.
- [20] R. Mills, K. Akhtar, "Tests of features of field-acceleration models for the extraordinary selective H Balmer  $\alpha$  broadening in certain hydrogen mixed plasmas," *Int. J. Hydrogen Energy*, Vol. 34, (2009), pp. 6465-6477.
- [21] R. L. Mills, B. Dhandapani, K. Akhtar, "Excessive Balmer  $\alpha$  line broadening of water-vapor capacitively-coupled RF discharge plasmas," *Int. J. Hydrogen Energy*, Vol. 33, (2008), pp. 802-815.
- [22] R. Mills, P. Ray, B. Dhandapani, "Evidence of an energy transfer reaction between atomic hydrogen and argon II or helium II as the source of excessively hot H atoms in RF plasmas," *Journal of Plasma Physics*, (2006), Vol. 72, Issue 4, pp. 469-484.

- [23] J. Phillips, C-K Chen, K. Akhtar, B. Dhandapani, R. Mills, "Evidence of catalytic production of hot hydrogen in RF generated hydrogen/argon plasmas," *International Journal of Hydrogen Energy*, Vol. 32(14), (2007), 3010-3025.
- [24] R. L. Mills, P. C. Ray, R. M. Mayo, M. Nansteel, B. Dhandapani, J. Phillips, "Spectroscopic study of unique line broadening and inversion in low pressure microwave generated water plasmas," *J. Plasma Physics*, Vol. 71, Part 6, (2005), pp. 877-888.
- [25] R. L. Mills, K. Akhtar, "Fast H in hydrogen mixed gas microwave plasmas when an atomic hydrogen supporting surface was present," *Int. J. Hydrogen Energy*, 35 (2010), pp. 2546-2555, doi:10.1016/j.ijhydene.2009.12.148.
- [26] M. Kuraica, N. Konjevic, "Line shapes of atomic hydrogen in a plane-cathode abnormal glow discharge," *Physical Review A*, Volume 46, No. 7, October (1992), pp. 4429-4432.
- [27] M. Kuraica, N. Konjevic, M. Platisa and D. Pantelic, *Spectrochimica Acta* Vol. 47, 1173 (1992).
- [28] I. R. Videnovic, N. Konjevic, M. M. Kuraica, "Spectroscopic investigations of a cathode fall region of the Grimm-type glow discharge," *Spectrochimica Acta*, Part B, Vol. 51, (1996), pp. 1707-1731.
- [29] S. Alexiou, E. Leboucher-Dalimier, "Hydrogen Balmer- $\alpha$  in dense plasmas," *Phys. Rev. E*, Vol. 60, No. 3, (1999), pp. 3436-3438.
- [30] S. Djurovic, J. R. Roberts, "Hydrogen Balmer alpha line shapes for hydrogen-argon mixtures in a low-pressure rf discharge," *J. Appl. Phys.*, Vol. 74, No. 11, (1993), pp. 6558-6565.
- [31] S. B. Radovanov, K. Dzierzega, J. R. Roberts, J. K. Olthoff, "Time-resolved Balmer-alpha emission from fast hydrogen atoms in low pressure, radio-frequency discharges in hydrogen," *Appl. Phys. Lett.*, Vol. 66, No. 20, (1995), pp. 2637-2639.
- [32] S. B. Radovanov, J. K. Olthoff, R. J. Van Brunt, S. Djurovic, "Ion kinetic-energy distributions and Balmer-alpha ( $H_\alpha$ ) excitation in  $Ar - H_2$  radio-frequency discharges," *J. Appl. Phys.*, Vol. 78, No. 2, (1995), pp. 746-757.
- [33] G. Baravian, Y. Chouan, A. Ricard, G. Sultan, *J. Appl. Phys.*, Vol. 61, (1987), p. 5249.
- [34] A. V. Phelps, *J. Phys. Chem. Ref. Data*, Vol. 21, (1992), p. 883.
- [35] C. Barbeau, J. Jolly, "Spectroscopic investigation of energetic atoms in a DC hydrogen glow discharge," *Journal of Physics, D, Applied Physics*, Vol. 23, (1990), pp. 1168-1174.
- [36] S. A. Bzenic, S. B. Radovanov, S. B. Vrhovac, Z. B. Velikic, and B. M. Jelenkovic, *Chem. Phys. Lett.*, Vol. 184, (1991), pp. 108-112.
- [37] E. L. Ayers, W. Benesch, "Shapes of atomic-hydrogen lines produced at a cathode surface," *Physical Review A*, Vol. 37, No. 1, (1988), pp. 194-199.

[38] W. Benesch, E. Li, "Line shapes of atomic hydrogen in hollow-cathode discharges," *Optic Letters*, Vol. 9, No. 8, (1984), pp. 338-340.

Figure 1. Experimental setup for the high-voltage pulsed discharge cell. The source emits its light spectra through an entrance aperture passing through a slit, with the spectra dispersed off a grazing-incidence grating onto a CCD detection system.

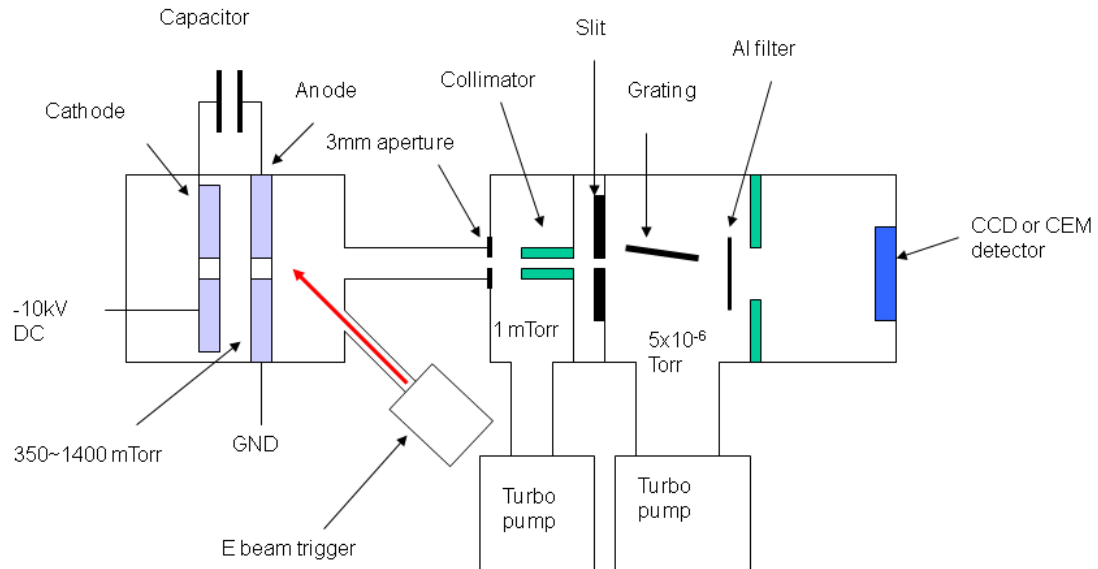
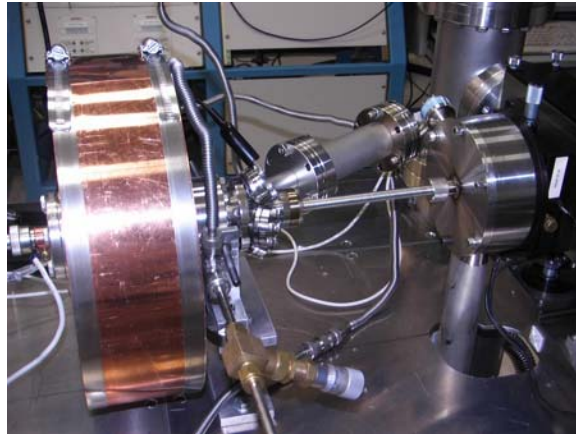
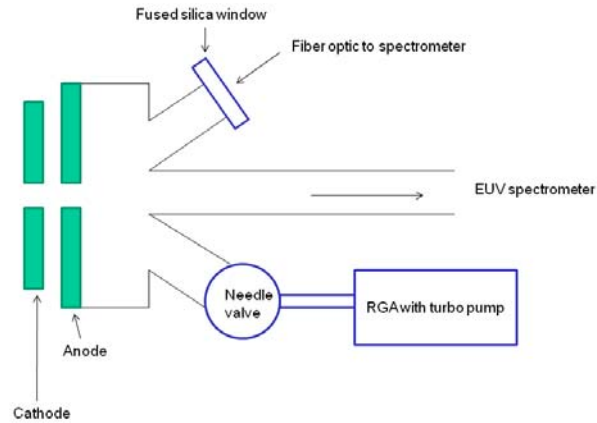


Figure 2. Photograph of the high-voltage pulsed discharge light source.

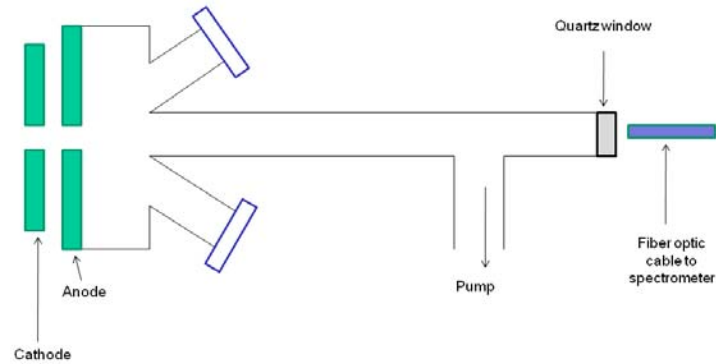


Figures 3A-B. Experimental setup for taking visible spectra of EUV discharges. (A) Port for recording emission of plasma and contaminant gases using the Ocean Optics spectrometer and for recording the W I 400.87 nm line emission using the Jobin Yvon Horiba 1250 M spectrometer. Also shown is the residual gas analyzer (RGA) mass spectrometer for identifying contaminants in EUV discharges. (B) Port for recording the widths of the 656.3 nm Balmer  $\alpha$  line and the 667.82 nm He I line using the Jobin Yvon Horiba spectrometer.



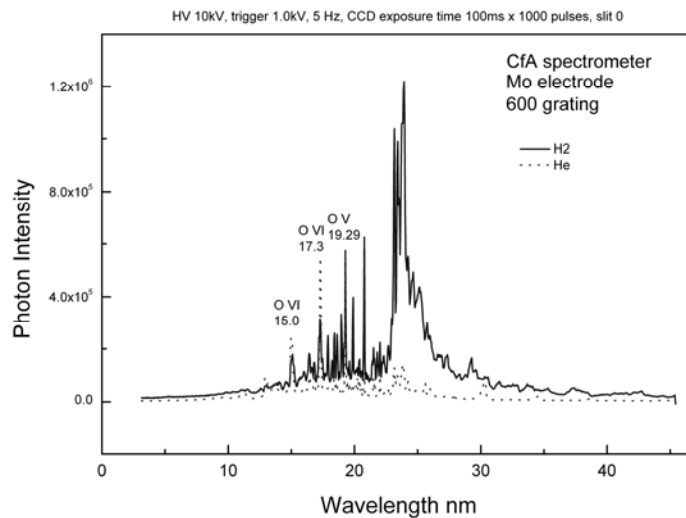
(A)

Set up for visible spectra at center of the pinch plasma

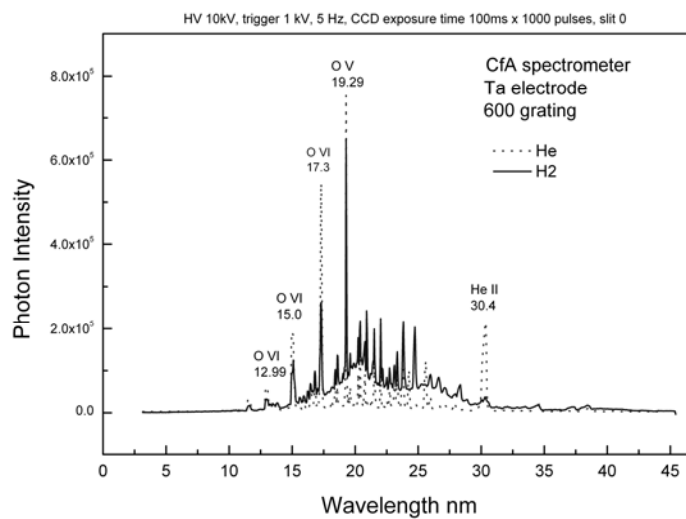


(B)

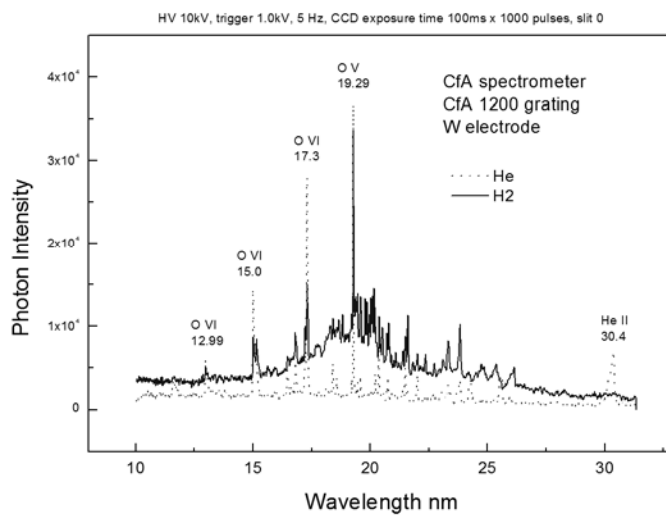
Figures 4A-D. Emission spectra (2.5–45 nm) comprising 1000 superpositions of electron-beam-initiated, high-voltage pulsed gas discharges in helium or hydrogen. Only known helium and oxygen ion lines were observed with helium in the absence of a continuum. Continuum radiation was observed for hydrogen only independent of the electrode, grating, spectrometer, or number of CCD image superpositions. (A) Helium and hydrogen plasmas maintained with Mo electrodes and emission recorded using the CfA EUV grazing incidence spectrometer with the BLP 600 lines/mm grating. (B) Helium and hydrogen plasmas maintained with Ta electrodes and emission recorded using the CfA EUV grazing incidence spectrometer with the BLP 600 lines/mm grating. (C) Helium and hydrogen plasmas maintained with W electrodes and emission recorded using the CfA EUV grazing incidence spectrometer with the CfA 1200 lines/mm grating. (D) Helium and hydrogen plasmas maintained with W electrodes and emission recorded using the CfA EUV grazing incidence spectrometer with the BLP 600 lines/mm grating.



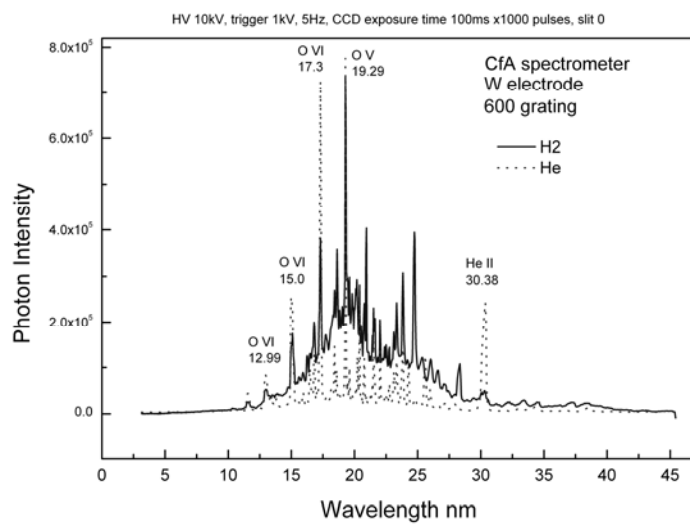
(A)



(B)

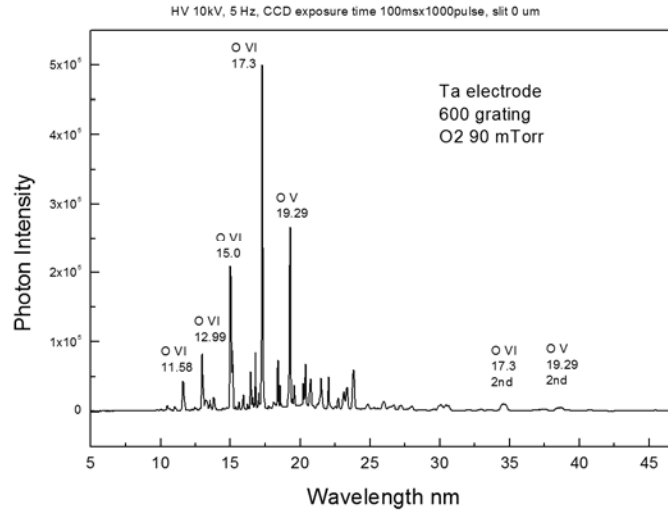


(C)

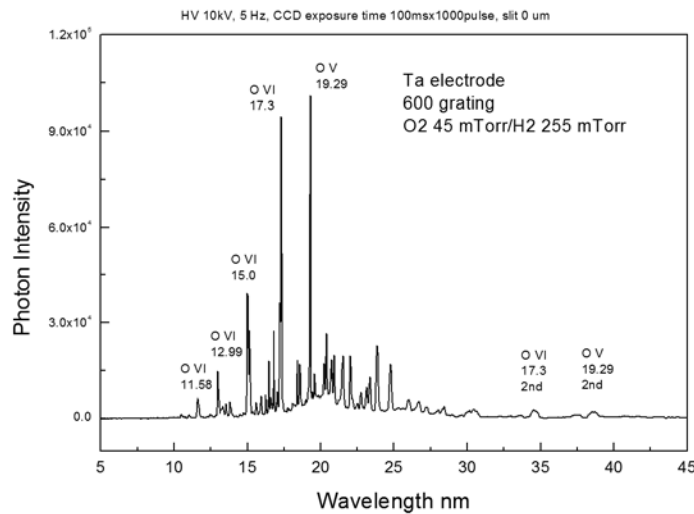


(D)

Figures 5A-B. Emission spectra (5–45 nm) of electron-beam-initiated, high-voltage pulsed discharges in oxygen and oxygen-hydrogen mixture maintained with Ta electrodes recorded using the EUV grazing incidence spectrometer with the 600 lines/mm grating and 1000 superpositions. (A) Pure oxygen plasma (90 mTorr) showing that only known oxygen ion lines were observed in the absence of a continuum. (B) Oxygen (45mTorr)-hydrogen (255 mTorr) plasma showing that a weak continuum was observed.



(A)



(B)

Figure 6. Emission spectra (5–50 nm) of electron-beam-initiated, high-voltage pulsed discharges in helium-hydrogen mixtures with W electrodes recorded by the EUV grazing incidence spectrometer using the 600 lines/mm grating and 1000 superpositions showing that the continuum radiation increased in intensity with increasing hydrogen pressure.

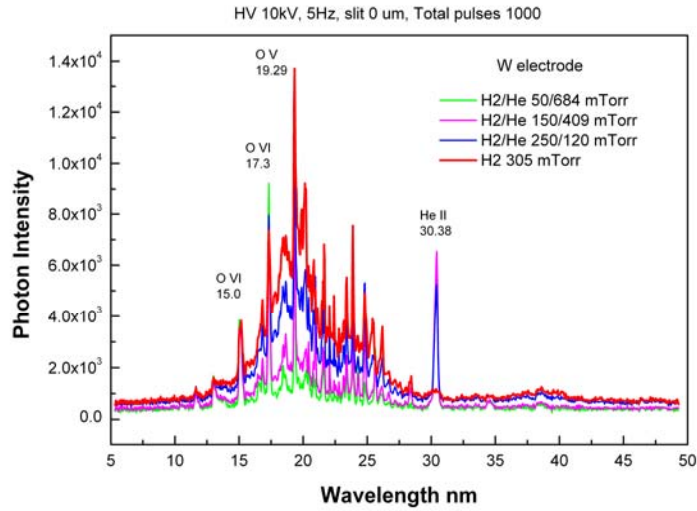


Figure 7. Emission spectrum (8–30 nm) of an electron-beam-initiated, high-voltage pulsed discharge in hydrogen using Ta electrodes recorded with the EUV grazing incidence spectrometer with the 600 lines/mm grating and 5000 superpositions having the CCD focused at 10 nm to enhance the sensitivity at the short-wavelength cutoff region. The cutoff of the continuum radiation is at about 10 nm.

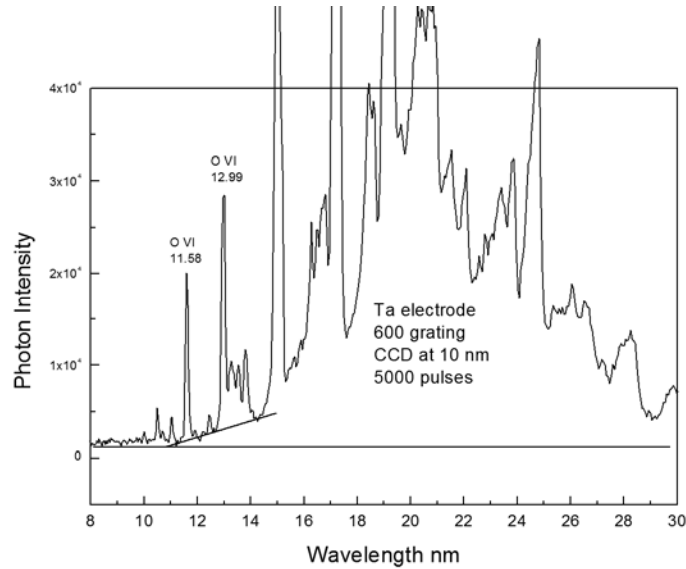


Figure 8. Emission spectrum (5–50 nm) of a self-triggered, high-voltage pulsed discharge in hydrogen maintained with Ta electrodes recorded with the EUV grazing incidence spectrometer with the 600 lines/mm grating using a liquid nitrogen cryotrap in the hydrogen gas line. The cutoff of the continuum radiation is at about 10 nm.

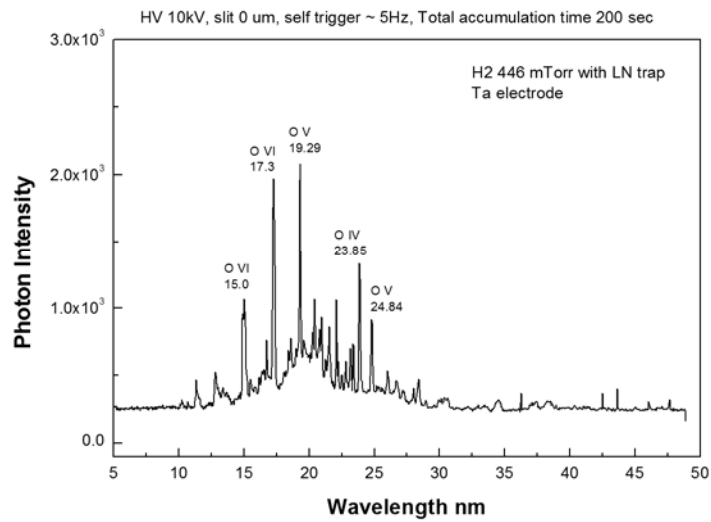
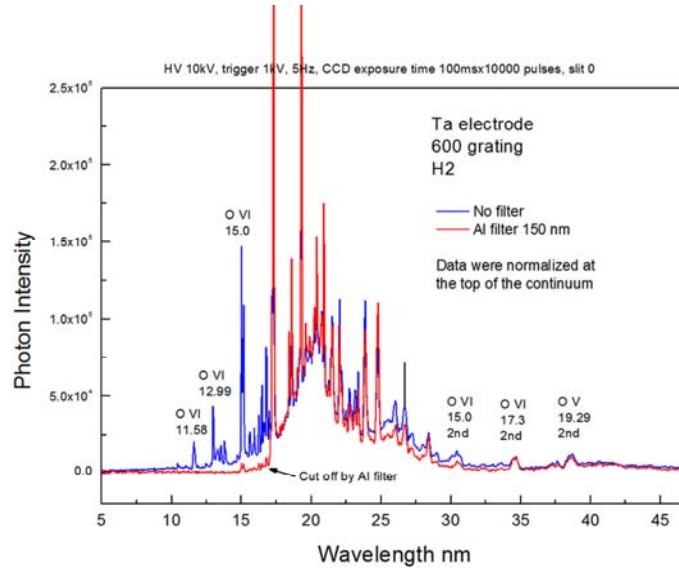
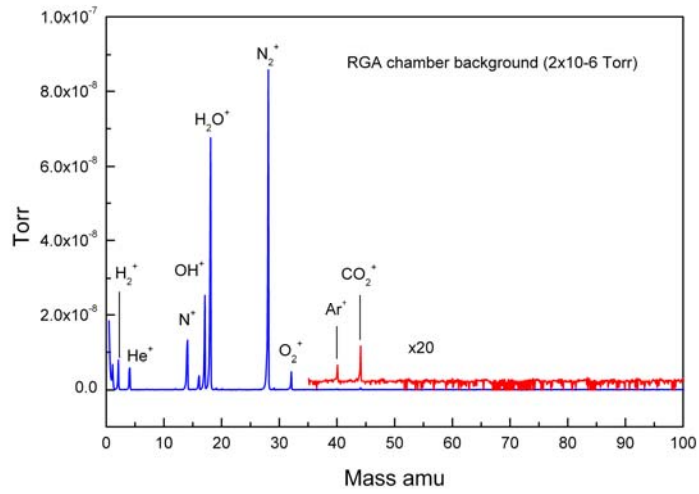


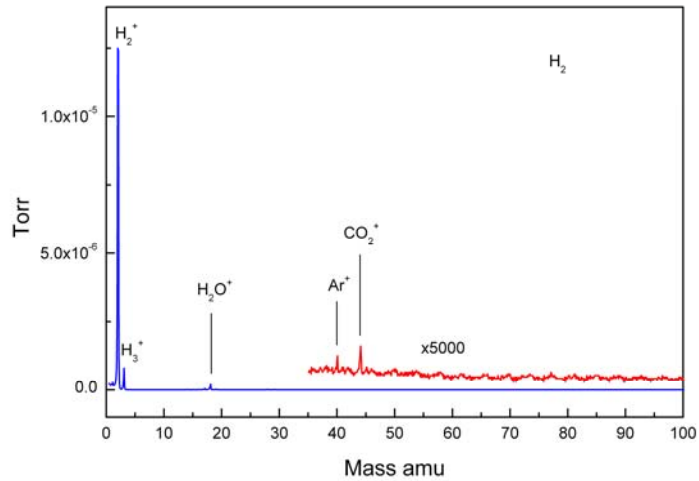
Figure 9. Emission spectra (5–45 nm) of electron-beam-initiated, high-voltage pulsed discharges in hydrogen maintained with Ta electrodes recorded by the EUV grazing incidence spectrometer using the 600 lines/mm grating and optionally an Al filter (150 nm thickness) showing that the continuum radiation from hydrogen plasmas had a cut-off at the 17 nm corresponding to the edge of the Al filter.



Figures 10A-B. (A) RGA mass spectrum on the mass spectrometer chamber background, showing only  $\text{H}_2^+$ ,  $\text{He}^+$ ,  $\text{N}^+$ ,  $\text{OH}^+$ ,  $\text{H}_2\text{O}^+$ ,  $\text{N}_2^+$ , and  $\text{O}_2^+$  and very trace amounts of  $\text{Ar}^+$  and  $\text{CO}_2^+$ . (B) Mass spectrum of  $\text{H}_2$  pinch plasma, showing mainly  $\text{H}_2^+$ ,  $\text{H}_3^+$ , and  $\text{H}_2\text{O}^+$  and very trace amounts of  $\text{Ar}^+$  and  $\text{CO}_2^+$ .

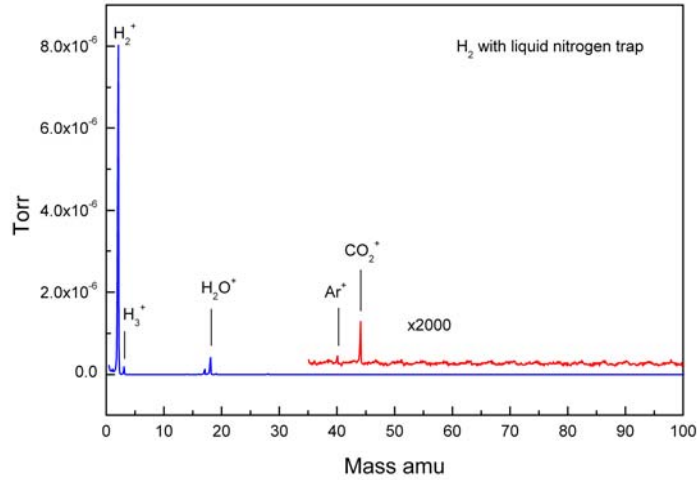


(A)

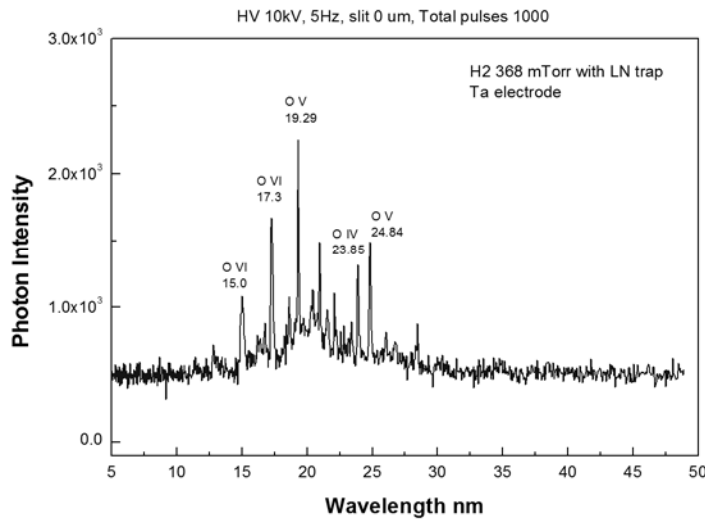


(B)

Figures 11A-B. (A) RGA mass spectrum of H<sub>2</sub> pinch plasma using a liquid nitrogen trap, showing mainly H<sub>2</sub><sup>+</sup>, H<sub>3</sub><sup>+</sup>, and H<sub>2</sub>O<sup>+</sup>. (B) Emission spectra (5–50nm) of an electron-beam-initiated, high voltage hydrogen discharge using a Ta electrode and a liquid-nitrogen cryotrap recorded with the EUV grazing incidence spectrometer with the 600 lines/mm grating, showing the presence of the continuum.

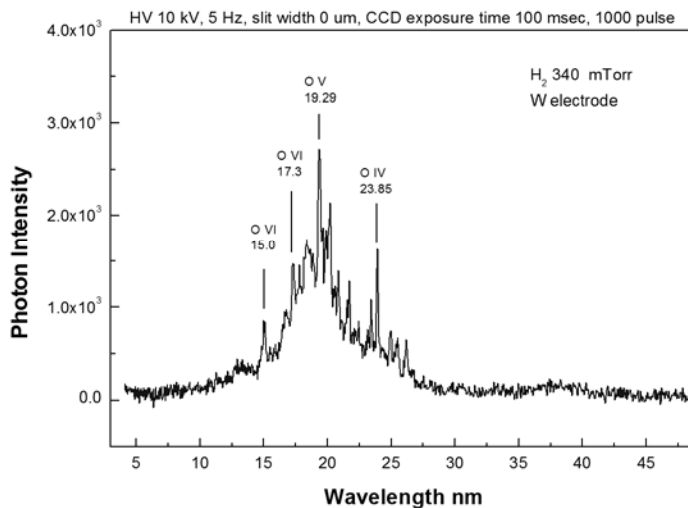


(A)

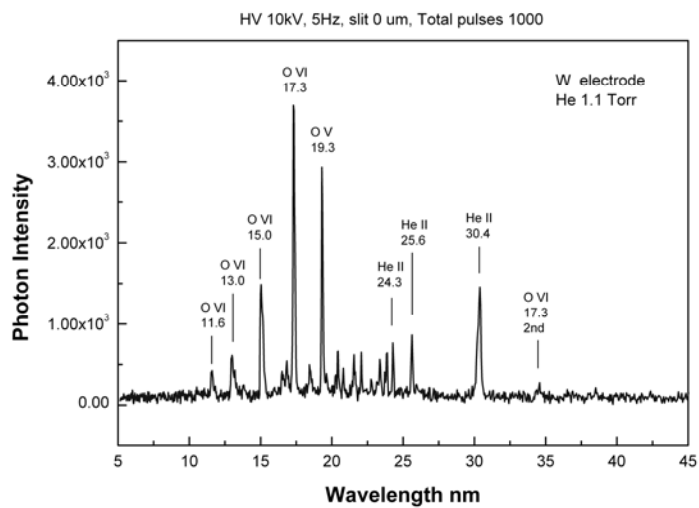


(B)

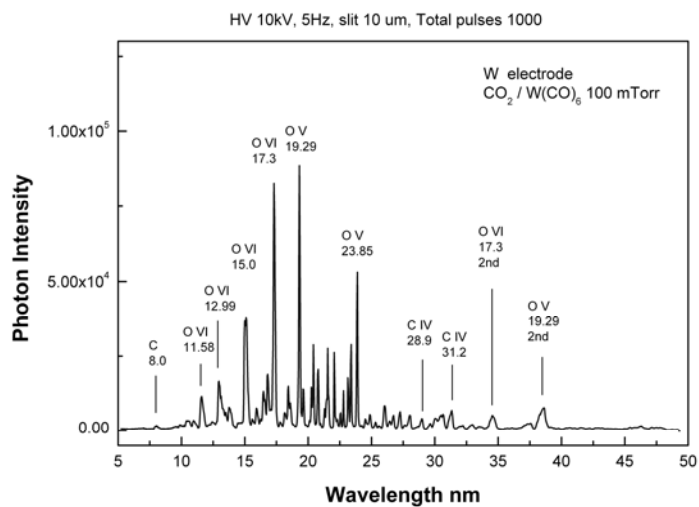
Figures 12A-H. Emission spectra (5–50 nm) of electron-beam-initiated, high-voltage pulsed discharges in H<sub>2</sub> compared to W(CO)<sub>6</sub> with CO<sub>2</sub> and N<sub>2</sub> plasma maintenance gas and control He, CO<sub>2</sub>, and N<sub>2</sub> plasmas maintained with W electrodes and recorded using the EUV grazing incidence spectrometer with the 600 lines/mm grating and 1000 superpositions. (A) Plasma of H<sub>2</sub> (340 mTorr) showing a continuum in the region of 10 to 30 nm. (B) Plasma of He (1.1 Torr) showing only known helium and oxygen lines in the absence of a continuum. (C) Plasma of W(CO)<sub>6</sub> vaporized in CO<sub>2</sub> (100 mTorr) showing only known oxygen and carbon lines in the absence of a continuum. (D) CO<sub>2</sub> (100 mTorr) plasma showing only known oxygen and carbon lines in the absence of a continuum. (E) Plasma of W(CO)<sub>6</sub> vaporized in N<sub>2</sub> (110 mTorr) showing only known oxygen, carbon, and nitrogen lines in the absence of a continuum. (F) N<sub>2</sub> (130 mTorr) plasma showing only known oxygen and nitrogen lines in the absence of a continuum. (G) Superposition of the (C) and (D) spectra showing that the presence of W in the plasma did not change the flat baseline. (H) Superposition of the (E) and (F) spectra showing that the presence of W in the plasma did not change the flat baseline.



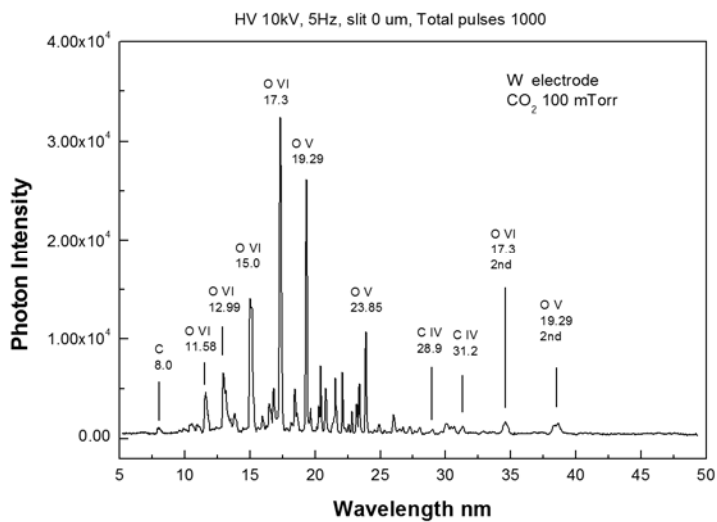
(A)



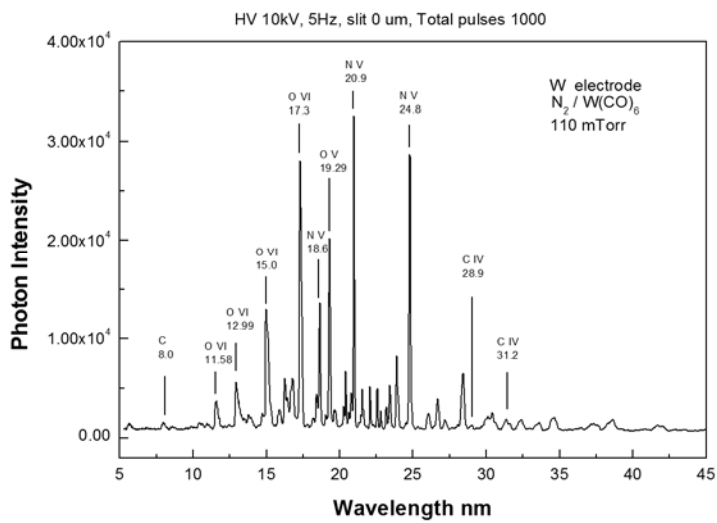
(B)



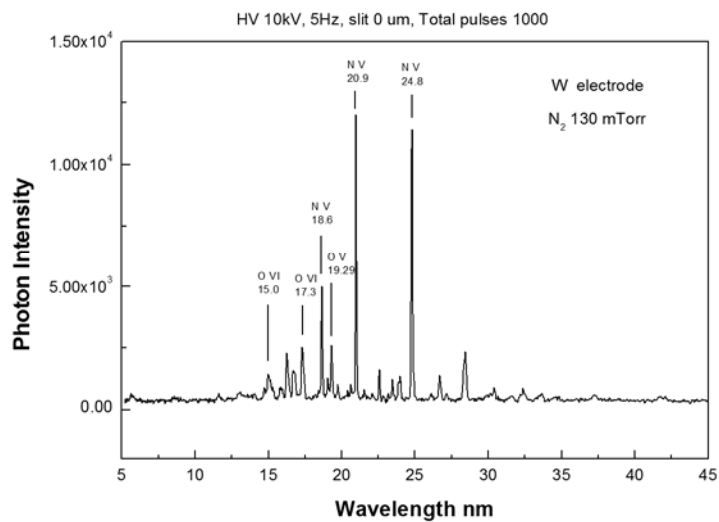
(C)



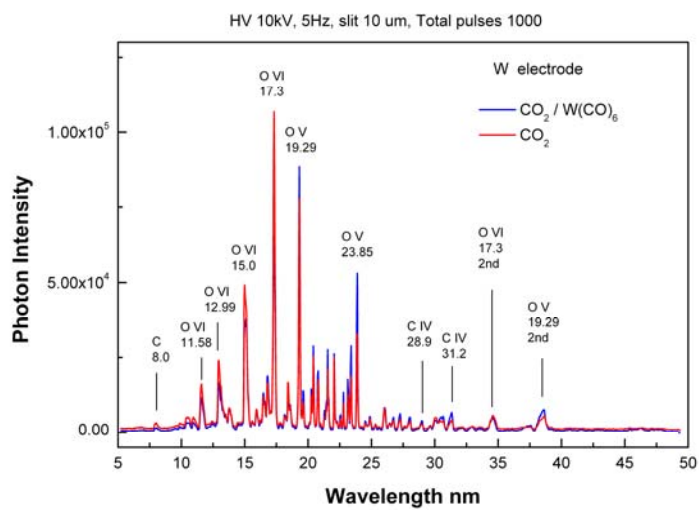
(D)



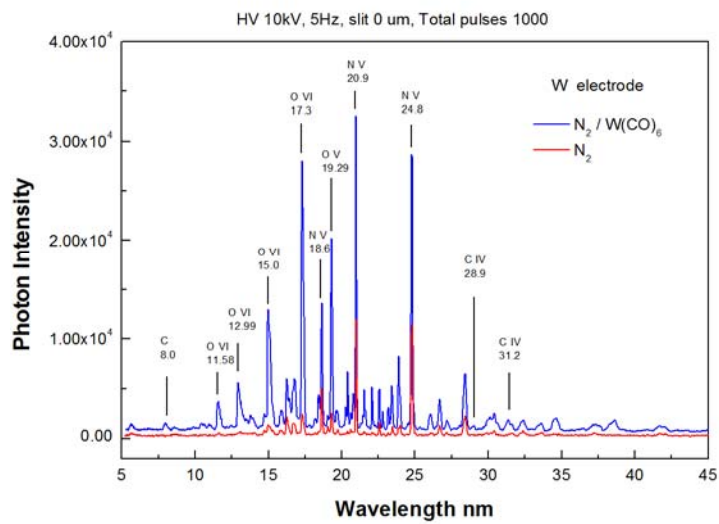
(E)



(F)

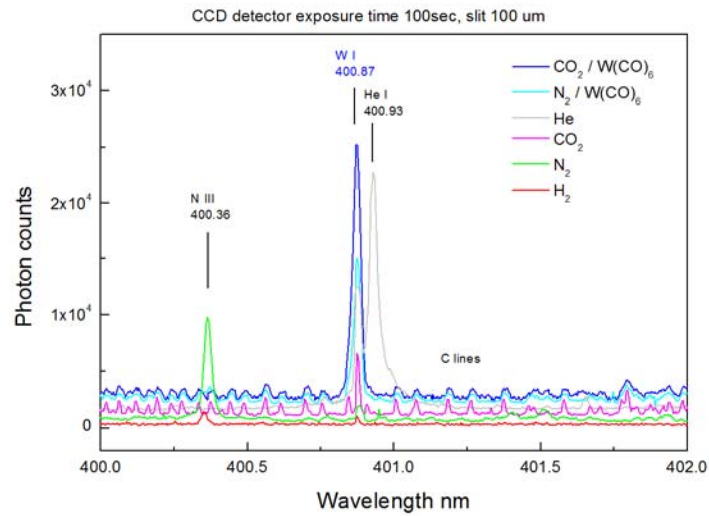


(G)

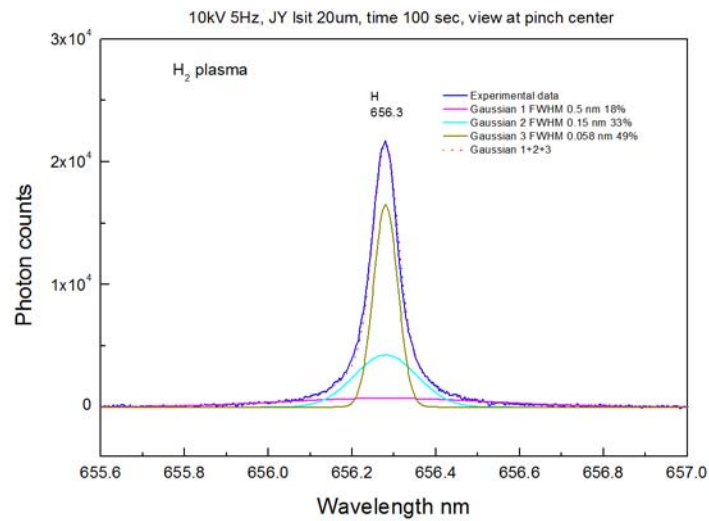


(H)

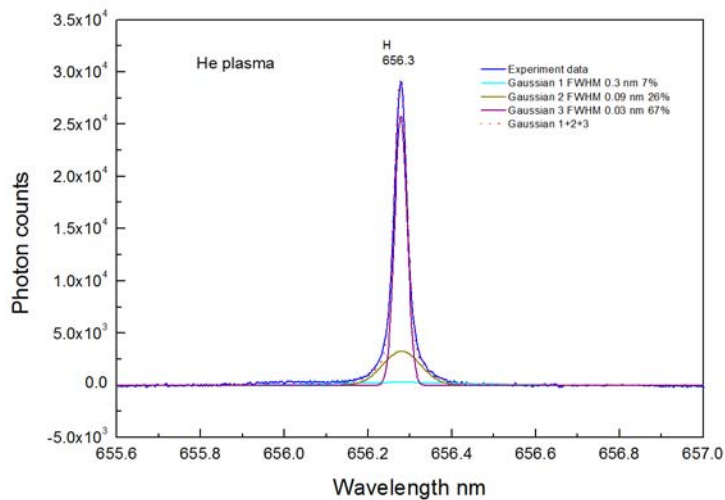
Figure 13. High-resolution visible emission spectra (400–402 nm offset for clarity) recorded with the Jobin Yvon Horiba 1250 M spectrometer on electron-beam-initiated, high-voltage pulsed plasmas maintained with W electrodes on a H<sub>2</sub> plasma that showed a continuum in the EUV region and plasmas of He, CO<sub>2</sub>, N<sub>2</sub>, W(CO)<sub>6</sub> in CO<sub>2</sub>, and W(CO)<sub>6</sub> in N<sub>2</sub> all of which showed no EUV continuum (Figure 12). The observed order of increasing intensity of the W I 400.87 nm line was H<sub>2</sub> < N<sub>2</sub> < CO<sub>2</sub> < He << W(CO)<sub>6</sub> in N<sub>2</sub> < W(CO)<sub>6</sub> in CO<sub>2</sub>. H<sub>2</sub> showed the lowest W emission consistent with its inefficiency as a sputtering species due to its low mass wherein the electrodes were the only source. The absence of continuum emission from all other sources having much greater W emission from the W electrodes and with added W from W(CO)<sub>6</sub> directly indicate that W is not the source of the continuum emission.



Figures 14A-B. The 656.3 nm Balmer  $\alpha$  line width recorded with the Jobin Yvon Horiba 1250 M spectrometer parallel to the electric field. Even though hydrogen ions were accelerated away from the detector, a symmetrical emission profile was observed indicating that the broadening was not dependent on the electric field. (A) Line profile recorded on a 200 mTorr H<sub>2</sub> pinch plasma showing a trimodal distribution wherein 18% and 33% of the hydrogen in the excited n = 3 state was fast with an average hydrogen atom energy of 98 eV and 8.8 eV, respectively, compared to 1.3 eV for the slow population. (B) Line profile recorded on a 500 mTorr He/trace H<sub>2</sub> pinch plasma showing a trimodal distribution wherein 7% and 26% of the hydrogen in the excited n = 3 state was fast with an average hydrogen atom energy of 35 eV and 3.2 eV, respectively, compared to 0.35 eV for the slow population.



(A)



(B)

Figure 15. The 667.816 nm He I line width recorded with the Jobin Yvon Horiba 1250 M spectrometer on a 500 mTorr He/trace H<sub>2</sub> pinch plasma wherein no broadening was observed even though the mass of He and hydrogen ions are similar indicating that the broadening was not dependent on the electric field. The He atoms' average thermal energy corresponding to a 0.025 nm Doppler half-width was 0.98 eV.

